

## Incommensurate Nature of the Antiferromagnetic Order in GdCu<sub>2</sub>

Koji Kaneko<sup>1,2\*</sup>, Chihiro Tabata<sup>1,2</sup>, Masato Hagihala<sup>1</sup>, Hiroki Yamauchi<sup>1</sup>, Masato Kubota<sup>1</sup>,  
Toyotaka Osakabe<sup>1</sup>, and Yoshichika Ōnuki<sup>3,4</sup>

<sup>1</sup>*Materials Sciences Research Center, Japan Atomic Energy Agency, Tokai, Naka, Ibaraki  
319-1195, Japan*

<sup>2</sup>*Advanced Science Research Center, Japan Atomic Energy Agency, Tokai, Naka, Ibaraki  
319-1195, Japan*

<sup>3</sup>*Faculty of Science, University of the Ryukyus, Nishihara, Okinawa 903-0213, Japan*

<sup>4</sup>*RIKEN Center for Emergent Matter Science, Wako, Saitama 351-0198, Japan*

A magnetic order in orthorhombic GdCu<sub>2</sub> was investigated via a single crystal neutron diffraction with thermal neutron. Magnetic peaks were observed at incommensurate positions described by the ordering vector  $\mathbf{q}=(\delta, 1, 0)$  with  $\delta=0.678$  at 4.6 K. This ordering vector is close to the commensurate one with  $\mathbf{q}_c=(2/3, 1, 0)$  reported earlier, but clearly deviates. The incommensurate nature of the magnetic order in GdCu<sub>2</sub> is further corroborated by the peak shift with temperature below  $T_N$ .

Trivalent Gd and divalent Eu ions show unique magnetic properties among rare-earth ions owing to an absence of orbital moment. Intermetallic compounds with Gd<sup>3+</sup> and Eu<sup>2+</sup> can be understood as spin magnetism mediated by RKKY interaction. Recently, topological magnetic orders, represented by magnetic skyrmion lattice, were discovered in Eu- and Gd-based compounds.<sup>1-6)</sup> Magnetic skyrmions in *f*-electron systems have characteristic properties such as short periodicity and anisotropy, compared with *d* electron systems, which can result from different formation mechanism.

An orthorhombic compound GdCu<sub>2</sub> attracts renewed interests in this respect. GdCu<sub>2</sub> undergoes an antiferromagnetic transition around 40 K.<sup>7,8)</sup> The magnetic structure in the ground state was reported to be a helical one characterized by the ordering vector  $\mathbf{q}_c=(2/3, 1, 0)$ .<sup>9)</sup> Because of the strong neutron absorption of Gd, hot neutron, a wavelength of  $\sim 0.5$  Å, was used to minimize attenuation. On the other hand, a short wavelength made it difficult to achieve high resolution in a momentum  $Q$  space. In order to get detailed insights into the magnetic

---

\*koji.kaneko@j-parc.jp

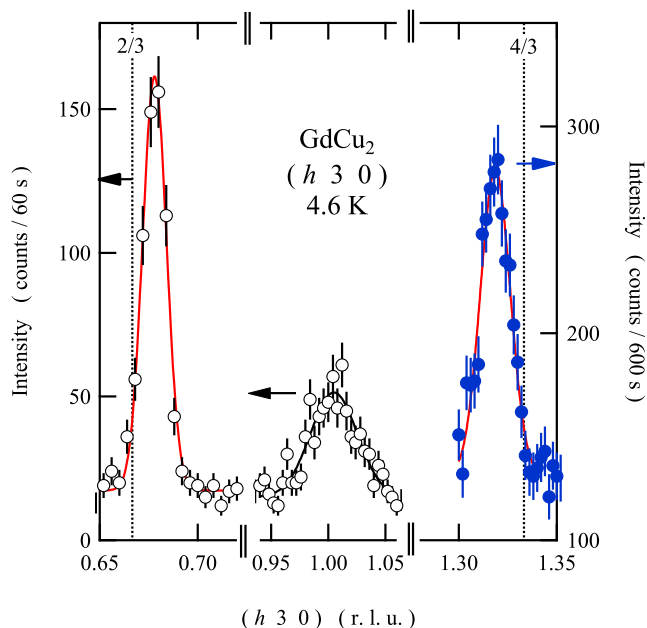


**Fig. 1.** (Color online) Scan along  $h$  through  $(1, 3, 0)$  collected at 4.6 K below  $T_N$ . Open circles are plotted with the left axis, while the closed circle uses the axis on the right. Dotted lines indicate commensurate peak positions with  $\delta=2/3$ .

order in  $\text{GdCu}_2$ , single crystal neutron diffraction experiment was performed using thermal neutron.

A single crystal sample of  $\text{GdCu}_2$  was grown by the Czochralski method as same as in Ref. 8. The plate-like sample of  $\sim 4 \times 4 \times 1.8 \text{ mm}^3$  with a plane normal to the  $b$ -axis was used in the present study. A single crystal neutron diffraction experiment was carried out on the thermal neutron triple-axis spectrometer TAS-2, installed at the T2-4 beam port in the guide hall of the research reactor JRR-3 in Tokai. Neutrons with a wavelength of  $2.359 \text{ \AA}$  were obtained and analyzed by pyrolytic graphite (PG) monochromator and analyzer. A collimation set of open-40'-S-40'-80' was employed with a PG filter before the sample. The sample was attached to a cold finger of a closed-cycle refrigerator to have  $(h k 0)$  in the horizontal scattering plane.

A linear absorption coefficient for  $\text{GdCu}_2$  with natural Gd is enormously large; roughly  $9 \mu\text{m}$  thickness will reduce neutron flux down to  $1/e$ . In order to avoid strong neutron attenuation, reflections close to the reciprocal  $(0 k 0)$  axis were chosen to have a reflection geometry for the present sample. Figure 1 shows a scan along  $h$  through  $(1 3 0)$  measured at 4.6 K below  $T_N$ . Three peaks were observed, which consists of a nuclear peak at center at  $(1 3 0)$  accompanied by satellite peaks on both sides. Note that the nuclear Bragg peak at  $(1 3 0)$  is

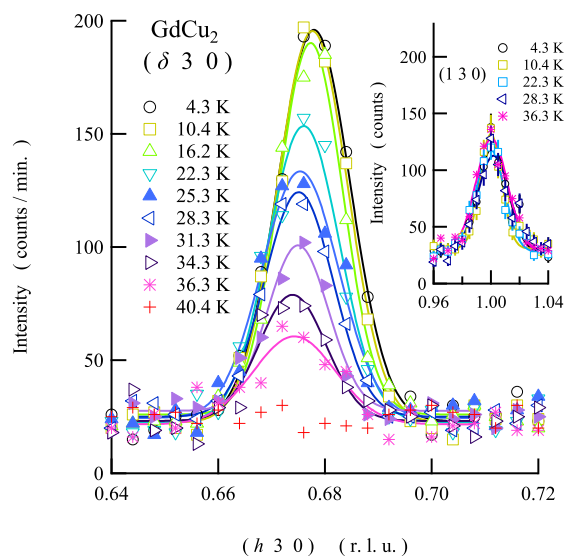


**Fig. 2.** (Color online) Representative line scan profiles along  $h$  through  $(\delta 3 0)$  measured at several temperatures below  $T_N$ . The inset shows line scan profile through nuclear peak at  $(1 3 0)$  recorded at selected temperatures.

forbidden for the symmetry  $Imma$ . As the central peak serves as a good reference to determine magnetic satellite peak positions precisely, the PG filter was partly removed and use  $\lambda/2$  to obtain the peak at  $(1 3 0)$ . In smaller  $h$  region, a sharp magnetic peak was observed at  $0.678(1)$  whose width corresponds to expected resolution of  $\sim 0.013$  r. l. u.. In contrast, a subtle, but clear magnetic peak was observed in larger  $h$  at  $1.323(1)$  plotted in the right axis, which needs 10 times longer counting time to obtain the similar statistics. By using the single parameter  $\delta$  to fit the both peak positions with respect to the nuclear peak,  $\delta$  was determined as  $0.678(1)$ . This is evidently smaller than  $2/3$ , which is indicated by broken lines in the figure. On the other hand, a scan along  $k$  confirms that the magnetic peak is centered at  $k=3$ , namely the  $k$  component is 1. The results indicate that the magnetic order in  $\text{GdCu}_2$  is not commensurate with  $\mathbf{q}_c=(2/3, 1, 0)$ , but has an incommensurate nature with  $\mathbf{q}=(\delta, 1, 0)$ .

This finding is also supported by its temperature dependence. Figure 2 shows the scan along  $h$  through  $(\delta 3 0)$  collected at several temperatures below  $T_N$ . With increasing temperature, the magnetic peak at the incommensurate position at  $h=0.678$  becomes weaker, and vanished at  $40.4$  K just above  $T_N$ . Concomitantly, the magnetic peak exhibits gradual peak shift to smaller  $h$  as temperature increases. This is contrast to the adjacent nuclear peak  $1 3 0$ , which stays at the same position as shown in the inset of Fig. 2.

Figure 3 summarizes the temperature variation of the peak position and intensity ob-

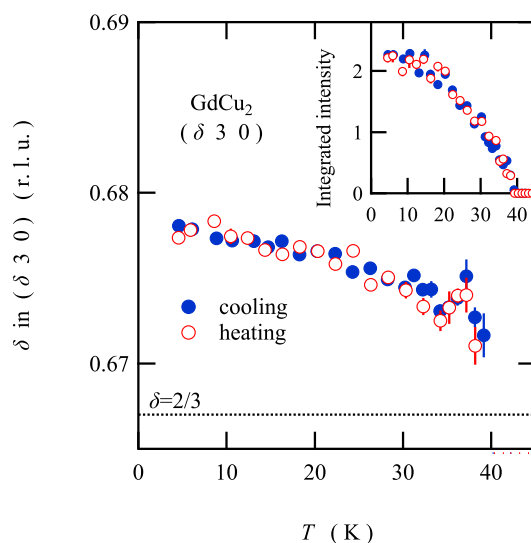


**Fig. 3.** (Color online) Magnetic peak position  $\delta$  in  $(\delta 3 0)$  as a function of temperature measured upon both heating and cooling. The inset shows temperature variation of the integrated intensity of the same magnetic reflection.

tained by a Gaussian fitting. Concerning the peak position, the peak at 0.678 at 4.6 K exhibits monotonous decrease with the temperature, and becomes 0.671 at 38.2 K. The peak positions  $\delta$  in the entire temperature range are larger than  $2/3$ , as indicated by the broken line in the figure. No visible difference exists between upon cooling and heating. A change of the peak position with temperature also supports an incommensurate nature of the transition in  $\text{GdCu}_2$ . The magnetic peak intensity shown in the inset develops gradually with decreasing temperature. No visible hysteresis was observed as in the peak position, consistent with a second-order nature of the magnetic transition in  $\text{GdCu}_2$ .

The present results reveal the incommensurate nature of the magnetic order in  $\text{GdCu}_2$ . The deviation from the commensurate order is small, 0.01 r.l.u. along  $a$ . Within the previous magnetic structure model, a small change in periodicity results in a slight reduction in pitch angle; the angle between neighboring magnetic moments along  $a$  is reduced from  $120^\circ$  to  $\sim 116^\circ$ . The lock-in transition to commensurate structure could not be seen in the present temperature range down to 4.6 K.

In general, neutrons with a short wavelength, 1 Å or less, are used to study high neutron absorbing material as absorption cross section follows so-called  $1/v$  law, where  $v$  corresponds to speed of neutron. Indeed, the high neutron absorption cross section of Gd, 58500 barns at a typical thermal-neutron wavelength 2.36 Å, can be suppressed to roughly 1/100 at hot neutron region at 0.5 Å. This suppression of neutron absorption enables quantitative structure

analysis as in the previous report.<sup>9)</sup> On the other hand, a short wavelength tends to result in a poor resolution in the  $Q$  space, in particular for low  $Q$  region. In other words, this setup is not ideal to determine precise periodicity as mentioned in Ref. 9. Whereas an accurate absorption correction and structural analysis could be problematic, a peak position and its variation with an external parameter can be tracked accurately with thermal neutron. A complementary use of both short- and long-wavelength neutrons leads to obtain a detailed picture of magnetic order.

In summary, the present study revealed that the antiferromagnetic order in orthorhombic  $\text{GdCu}_2$  can be described with the incommensurate ordering vector with  $\mathbf{q}=(\delta, 1, 0)$  with  $\delta=0.678$  at 4.6 K. The gradual change of  $\delta$  with the temperature also supports an incommensurate nature of the transition in  $\text{GdCu}_2$ .

### **Acknowledgment**

We thank Y. Shimojo and M. Sasaki for their support on neutron scattering experiments. This work was supported by JSPS KAKENHI Grants Nos. JP20H01864, JP21H01027, JP21H04987, and No. JP19H04408.

## References

- 1) M. Kakihana, D. Aoki, A. Nakamura, F. Honda, M. Nakashima, Y. Amako, S. Nakamura, T. Sakakibara, M. Hedou, T. Nakama, and Y. Ōnuki, *J. Phys. Soc. Japan* **87**, 023701 (2018).
- 2) K. Kaneko, M. D. Frontzek, M. Matsuda, A. Nakao, K. Munakata, T. Ohhara, M. Kakihana, Y. Haga, M. Hedou, T. Nakama, and Y. Ōnuki, *J. Phys. Soc. Japan* **88**, 013702 (2019).
- 3) M. Hirschberger, T. Nakajima, S. Gao, L. Peng, A. Kikkawa, T. Kurumaji, M. Kriener, Y. Yamasaki, H. Sagayama, H. Nakao, K. Ohishi, K. Kakurai, Y. Taguchi, X. Yu, T.-h. Arima, and Y. Tokura, *Nat. Commun.* **10**, 5831 (2019).
- 4) T. Kurumaji, T. Nakajima, M. Hirschberger, A. Kikkawa, Y. Yamasaki, H. Sagayama, H. Nakao, Y. Taguchi, T.-h. Arima, and Y. Tokura, *Science* **365**, 914 (2019).
- 5) N. D. Khanh, T. Nakajima, X. Yu, S. Gao, K. Shibata, M. Hirschberger, Y. Yamasaki, H. Sagayama, H. Nakao, L. Peng, K. Nakajima, R. Takagi, T.-h. Arima, Y. Tokura, and S. Seki, *Nat. Nanotechnol.* **15**, 444 (2020).
- 6) R. Takagi, N. Matsuyama, V. Ukleev, L. Yu, J. S. White, S. Francoual, J. R. L. Mardegan, S. Hayami, H. Saito, K. Kaneko, K. Ohishi, Y. Ōnuki, T.-h. Arima, Y. Tokura, T. Nakajima, and S. Seki, *Nat. Commun.* **13**, 1472 (2022).
- 7) N. H. Luong, J. Franse, and T. D. Hien, *J. Magn. Magn. Mater.* **50**, 153 (1985).
- 8) A. Koyanagi, Y. Yoshida, Y. Kimura, R. Settai, K. Sugiyama, and Y. Ōnuki, *J. Phys. Soc. Japan* **67**, 2510 (1998).
- 9) M. Rotter, A. Lindbaum, E. Gratz, G. Hilscher, H. Sassik, H. E. Fischer, M. T. Fernandez-Diaz, R. Arons, and E. Seidl, *J. Magn. Magn. Mater.* **214**, 281 (2000).